Applied Catalysis B: Environmental 123–124 (2012) 193–199

Contents lists available at SciVerse ScienceDirect

Applied Catalysis B: Environmental

journal homepage: www.elsevier.com/locate/apcatb

Ag-AgCl/WO_3 hollow sphere with flower-like structure and superior visible photocatalytic activity

Bowen Ma, Jianfeng Guo, Wei-Lin Dai*, Kangnian Fan

Department of Chemistry and Shanghai Key Laboratory of Molecular Catalysis and Innovative Materials, Fudan University, Shanghai 200433, PR China

ARTICLE INFO

Article history:
Received 11 January 2012
Received in revised form 18 April 2012
Accepted 22 April 2012
Available online 26 April 2012

Keywords:
Photocatalyst
Ag-AgCl/WO_3
Plasmon resonance
photodegradation
4-chlorophenol

ABSTRACT

In this work, we describe an effective route to synthesize Ag-AgCl/WO_3 hollow sphere with flower-like structure, which displayed excellent visible light response photocatalytic activity and recycling ability for the degradation of 4-chlorophenol. Its high photocatalytic activity can be attributed to the surface plasmon resonance effect of Ag nanoparticles, which were highly dispersed on the surface of Ag-AgCl/WO_3. N_2 adsorption and desorption isotherm spectra, X-ray diffraction, X-ray photoelectron spectroscopy, and electron microscopy were used to determine the correlation between the micro-structure and the catalytic properties of the as-prepared photocatalysts.

1. Introduction

To date, many kinds of semiconductor metal oxides have been studied. Among them, TiO_2 has been recognized as an interesting semiconductor material for a long time, owing to its potential in photoelectron-chemical solar-energy conversion with a high degree of efficiency, photochemical stability, non-toxic nature and low cost [1,2]. Photodegradation of various pollutants [3–5] and the destruction of bacteria [6,7] using TiO_2 photocatalyst has been a very popular topic of research in recent years. However, further studies on TiO_2 photocatalysts in the practical application were hindered by the main drawbacks of the low quantum yields and the lack of visible-light utilization. It is highly desirable to develop a photocatalyst that can harness visible light with high efficiency under normal sunlight conditions.

In the past, the dominant factors to affect photocatalysis have been explored so as to enable photocatalysts to be active in the visible light irradiation, including phase/morphological control, doping, surface sensitization, noble metal loading, and the use of composite materials [8–15]. Composite semiconductors have been reported to be potential as photocatalysts because they can reduce the recombination of photogenerated electrons and holes [16,17], and therefore can increase the lifetime of the charge carriers and enhance the quantum yield [18].

Noble metal nanoparticles (NPs) exhibit characteristic optical and physical properties that are substantially different from those of the corresponding bulk material. Particularly, silver NPs show efficient plasmon resonance in the visible region. On the basis of this character, Awazu et al. [19] developed a preparation method for plasmonic photocatalyst, during which TiO_2 was deposited on the surface of SiO_2@Ag NPs to prevent the oxidation of Ag by direct contact with TiO_2. Thus, this plasmonic photocatalyst exhibits greater catalytic activity. Recently, Wang et al. [20,21] synthesized Ag@AgCl and Ag@AgBr plasmonic photocatalysts through ion exchange and photoreduction method, which showed excellent photocatalytic activity under visible light irradiation. It is reported that silver halide, generally considered as photosensitive materials, can coexist stably with Ag NPs during the whole photocatalytic reaction process. Kakuta et al. [22] also observed that Ag^0 species could contribute to the smooth separation of electron–hole pairs on the AgBr/SiO_2 NPs and enable it to catalyze H_2 production from alcohol radicals. Later, a bunch of this kind of plasmonic photocatalyst has been prepared and studied. Hu et al. [23] have prepared AgI/TiO_2 by the deposition–precipitation method with high efficiency for the degradation of non-biodegradable azodyes under visible light irradiation. AgBr/Al-MCM-41 was prepared by Rodrigues et al. [24] with high activity for the photooxidation of acetaldehyde in the gas phase under visible and UV light. Hu et al. [25] prepared a composite material with Ag-AgI supported on mesoporous alumina (Ag-AgI/Al_2O_3) and put forth the mechanism of plasmon-induced photocatalytic reaction. In our previous work, we prepared super-paramagnetic core–shell Fe_3O_4@SiO_2 NPs through solvothermal and sol–gel method, and

* Corresponding author. Tel.: +86 21 55664678; fax: +86 21 55665572.
E-mail address: wldai@fudan.edu.cn (W.-L. Dai).

0926-3373/$ – see front matter © 2012 Elsevier B.V. All rights reserved.
http://dx.doi.org/10.1016/j.apcatb.2012.04.029

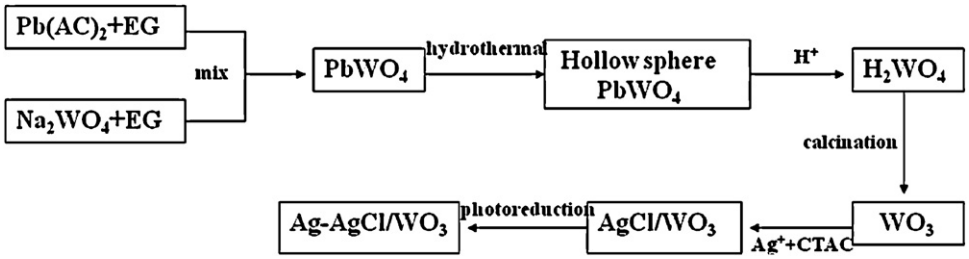

Scheme 1. The schematic diagram of the preparation procedure of Ag-AgCl/WO_3 photocatalyst.

then fabricated Ag-AgI/Fe_3O_4@SiO_2 plasmonic photocatalyst via deposition–precipitation and photoreduction method [26]. And Ag/AgCl@ cotton-fabric plasmonic photocatalyst has also been synthesized by a facile method, which exhibits excellent stability for the decomposition of RhB and convenience in the separation and recovery of the catalyst from the solution [27].

Herein, we applied tungsten oxide (WO_3) into our catalyst to form the Ag-AgCl/WO_3 composite catalyst. Nanostructured WO_3 [28–35] is of great interest due to its broad range of applications, such as gas sensors, photocatalysts, electrochromic devices, field-emission devices, and solar-energy devices. In addition, WO_3 turns out to be an interesting candidate for visible light sensitive photocatalysts. WO_3 is an *n*-type semiconductor with an indirect bandgap of 2.7 eV. This material is chemically stable in acid media and cannot be further oxidized [36]. WO_3 nanoparticles have also been studied for degradation of organic dyes [37]. In the present work, it is found that the Ag-AgCl/WO_3 hollow sphere photocatalyst has the advantages both of a plasmon effect and a composite photocatalyst. It exhibits high efficiency in degradation of 4-chlorophenol (4-CP), and is photostable under repeated use.

2. Experimental

2.1. Preparation

2.1.1. Preparation of the hollow sphere $PbWO_4$

The $PbWO_4$ precursors were synthesized using a solvothermal process [28]. In a typical procedure, 1.51 g of $Pb(AC)_2{\cdot}H_2O$ and 1.31 g of Na_2WO_4 were respectively dissolved in two sets of 50 mL of aqueous ethylene glycol solution. Then the as-obtained solutions were mixed under vigorous magnetic stirring at room temperature and white precipitates were generated. The resulting suspension was further stirred for 10 min and then was transferred into a Teflon-lined stainless steel autoclave, followed by heat treatment at 160 °C for certain time. After cooling to room temperature, the products was filtered, washed three times with alcohol/water mixture (v/v = 1:1) and then dried in air at 80 °C overnight.

2.1.2. Preparation of the hollow sphere WO_3

To get hierarchical WO_3 hollow structures, the $PbWO_4$ precursors with different morphologies were firstly immersed in 100 mL of 4 M HNO_3 solution for 48 h. Then the products were filtered, washed with distilled water, and dried in air. After then, the acid-treated products were calcined in a furnace at 500 °C for 2 h in air.

2.1.3. Preparation of Ag-AgCl/WO_3

The photocatalyst were prepared by the deposition–precipitation–photoreduction method. 0.5 g of as-prepared hollow sphere WO_3 and 0.12 g of hexadecyl trimethyl ammonium chloride (CTAC) were added into 100 mL of distilled water and the mixture was stirred at room temperature for 30 min. The aqueous solution of $AgNO_3$ was added into the above mixture. After being stirred magnetically for 20 min, the above mixture was irradiated with a 4 × 8 W ultraviolet lamp (λ = 254 nm) for certain minutes to reduce partial Ag^+ ions in the AgCl particles to Ag^0 species by photochemical decomposition of AgCl. The as-prepared samples with different photoreduction time were named as XAg-AgCl/WO_3, where X stands for the irradiation time in minutes. After that, the catalysts were collected, washed with distilled water and dried at 80 °C for 24 h in dark. Finally, the as-prepared products were calcined in air at 300 °C for 3 h to obtain the Ag-AgCl/WO_3 hollow sphere. Scheme 1 describes the detailed preparation process.

2.2. Characterization

XRD patterns of the as-prepared samples (2θ ranges from 10° to 70°) were recorded at room temperature with scanning speed of 2° min^{-1} using Cu Kα radiation (λ = 0.154 nm) from a 40 kV X-ray source (Bruker D8 Advance). Diffuse reflectance spectroscopy was performed using a SHIMADZU UV-2450 instrument with a collection speed of 40 nm min^{-1} using $BaSO_4$ as the reference. Transmission electron micrographs (TEM) were obtained using a JEOL 2011 microscope operating at accelerating voltage of 200 kV. X-ray photoelectron spectroscopy (XPS) measurements were performed on a PHI 5000C ESCA System with Mg Kα source at 14.0 kV and 25 mA. All the binding energies were referenced to the contaminant C1s peak at 284.6 eV of the surface adventitious carbon. Scanning electron micrographs (SEM) were obtained using a PHILIPS XL 30 microscope operating at accelerating voltage of 20 kV.

2.3. Evaluation of photocatalytic activity

Photocatalytic experiments were performed in a beaker placed under the lamp bracket, containing aqueous suspensions of 4-CP (100 mL, 10 mg L^{-1}) and 50 mg of catalyst powder. The light source was a 125 W metal halide lamp (Philips) equipped with wavelength cutoff filters for $\lambda \leq 420$ nm and focused on the beaker. Prior to the irradiation, the suspension was ultrasonicated for 10 min and then stirred in dark for 30 min to achieve the adsorption/desorption equilibrium. After turning on the lamp, 2 mL of suspension was sampled at certain time intervals and centrifuged by centrifuge (Shanghai Anting Scientific Instrument Factory, China) at 13,000 rpm for 10 min to remove the particles. The upper clear liquid was analyzed by recording the characteristic absorption peak of 4-CP at 280 nm to calculate the concentration of the compounds according to the work curve previously drawn.

3. Results and discussion

3.1. Catalysts characterization

Fig. 1 shows the XRD patterns of WO_3 and the Ag-AgCl/WO_3 with different photoreduction duration. All the diffraction peaks

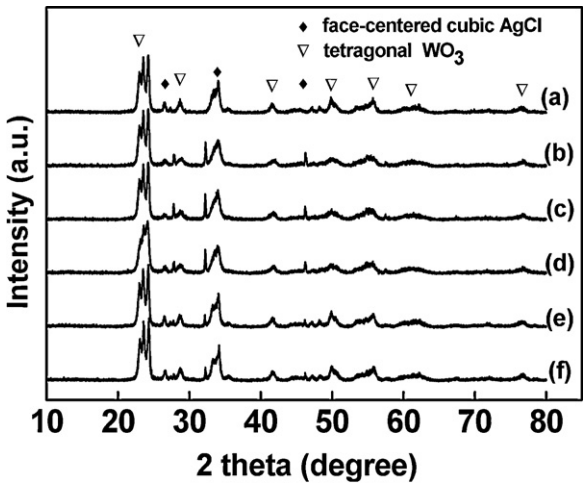

Fig. 1. XRD patterns of Ag-AgCl/WO_3 with different photo-reduction time (a) WO_3; (b) 10Ag-AgCl/WO_3; (c) 20Ag-AgCl/WO_3; (d) 30Ag-AgCl/WO_3; (e) 40Ag-AgCl/WO_3; (f) 50Ag-AgCl/WO_3.

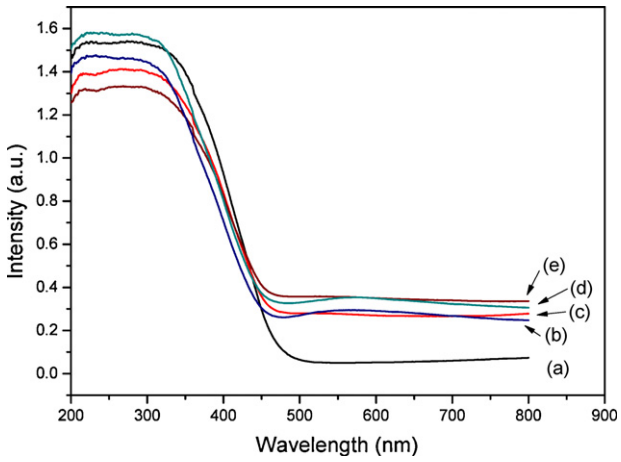

Fig. 3. UV–vis DRS spectra of Ag-AgCl/WO_3-500 with different photo-reduction time (a) WO_3-500; (b) 10Ag-AgCl/WO_3-500; (c) 20Ag-AgCl/WO_3-500; (d) 30Ag-AgCl/WO_3-500; (e) 40Ag-AgCl/WO_3-500.

can be indexed as the tetragonal WO_3, and cubic phase AgCl respectively, which are marked clearly in Fig. 1. In the patterns, the peak $2\theta = 32.2^\circ$ was indexed to the (2 0 0) plane of cubic AgCl and the peak $2\theta = 46.2^\circ$ was corresponded to the (2 2 0) plane. As shown, the characteristic peaks belonging to tetragonal WO_3 in the catalysts Ag-AgCl/WO_3 were detected, indicating that the loading of Ag/AgCl on the WO_3 did not destroy the phase structure of the support. However, from the figure, the diffraction peaks attributed to cubic Ag could not be easily observed, suggesting that the Ag nanoparticles were uniformly dispersed on the surface of WO_3 and the size of the silver particles was too small to be detected. In addition, with the increase of the photoreduction duration, the peaks corresponded to AgCl became weaker, indicating that during the photoreduction duration, AgCl was decomposed to metallic Ag species under UV light irradiation.

The specific surface area of the samples WO_3-500 and 30Ag-AgCl/WO_3 was measured using the BET method with N_2 adsorption and desorption at $-196\,^\circ C$ and N_2 adsorption–desorption isotherms curves of photocatalysts WO_3-500 and 30Ag-AgCl/WO_3-500 are shown in Fig. 2. It is found that there was no obvious difference before and after the deposition of Ag/AgCl on WO_3. The N_2 adsorption–desorption isotherms curves of photocatalysts are

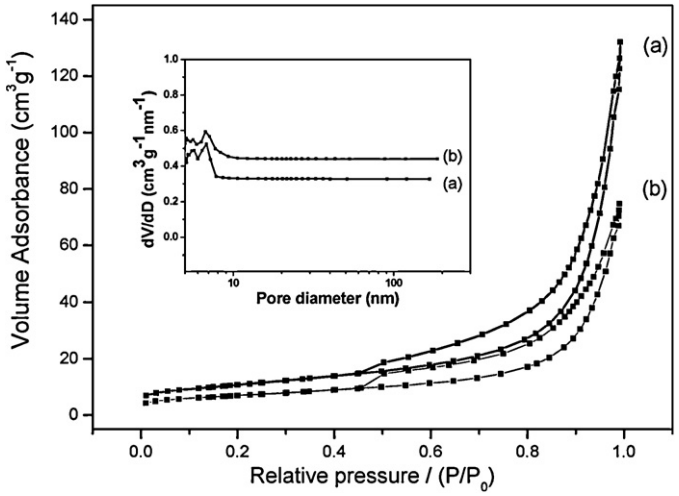

Fig. 2. N_2 adsorption/desorption isotherms curves of photocatalyst WO_3-500 (a) and 30Ag-AgCl/WO_3-500(b).

type IV isotherms. The pore-size distribution was also very similar for these two materials. N_2 adsorption and desorption results indicated that the introduction of Ag/AgCl had little effect on the structural properties of the WO_3-500 support.

Fig. 3 shows the UV–vis diffuse-reflectance spectra (DRS) of the as-prepared catalysts. Comparing with the WO_3-500, the series of Ag-AgCl/WO_3-500 photocatalysts did not have an obviously stronger absorption in the region of ultraviolet light. However, the series of Ag-AgCl/WO_3-500 photocatalysts exhibited broad absorption in the 500–800 nm region of visible light, owing to the surface plasmon resonance (SPR) effect of Ag NPs, which were produced by the photo-reduction of AgCl. When the wavelength of the incident light is much greater than the diameter of silver NPs, the electromagnetic field across each entire silver NP is essentially uniform. With the oscillations in that electromagnetic field, the weakly bound electrons of the silver nanoparticles respond collectively, giving rise to the plasmonic state. When the incident light frequency matches the plasmonic oscillation frequency, the incident light will be absorbed, resulting in surface plasmon absorption. When the catalysts were irradiated with visible light, some Ag nanoparticles on the surface of the catalysts might become larger as a result of the reduction of AgCl. Therefore, the shapes and diameters of the Ag NPs vary over a large range. As a result, the frequency of their plasmonic oscillations covers a wide range, permitting Ag/AgCl and Ag/AgCl@WO_3 to absorb visible and UV light over a wide range. As the duration of photo-reduction increased, Ag NP contents increased correspondingly, resulting in the enhanced intensity of visible light response from 10Ag-AgCl/WO_3-500 to 40Ag-AgCl/WO_3-500.

SEM images of these H_2WO_4 and 30Ag-AgCl/WO_3 spheres calcinated at $500\,^\circ C$ were shown in Fig. 4. As shown, before and after calcinations, the samples kept the unique shape and the hollow sphere was not destroyed. Due to the structure of hollow sphere, the incident lights could be reflected repeatedly and consequently enhanced the utilization efficiency of light, which might improve the photocatalytic activity of the as-prepared catalysts.

The TEM images and EDX result of 30Ag-AgCl/WO_3 photocatalyst were presented in Fig. 5. The Ag nanoparticles with average diameter of about 10 nm were uniformly dispersed on the surface of WO_3. From the EDX result, it is found that some particles were pure silver, and other particles were ascribed to AgCl. It would be the direct evidence to prove the Ag/AgCl nanoparticles co-dispersed on the surface of WO_3. Fig. 6 shows the typical XPS spectra of 30Ag-AgCl/WO_3. As 10Ag-AgCl/WO_3, 20Ag-AgCl/WO_3, and 40Ag-AgCl/WO_3 have spectra similar to that of 30Ag-AgCl/WO_3, they

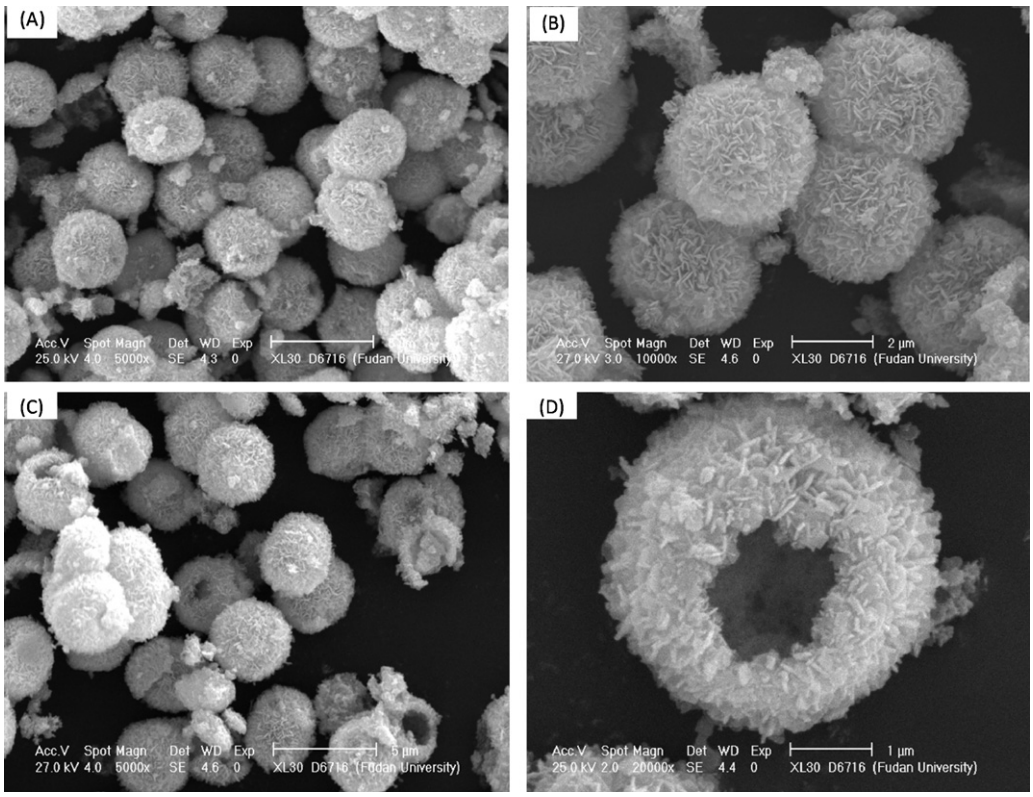

Fig. 4. SEM images of H_2WO_4 (A) and 30Ag-AgCl/WO_3 (B), (C) and (D) in different magnification.

were not shown here. In addition, XPS results (Fig. 6) could demonstrate the coexistence of Ag and AgCl on the surface of WO_3. As shown in Fig. 6A, the 30Ag-AgCl/WO_3 catalyst contained Ag and Cl elements with a molar ratio of 3:2 that is higher than the stoichiometric ratio in AgCl (1:1), indicating the existence of excessive Ag on the surface.

In Fig. 6B, the Ag 3d spectra of 30Ag-AgCl/WO_3 consisted of two individual peaks attributed to Ag $3d_{3/2}$ and Ag $3d_{5/2}$. The peak of Ag $3d_{3/2}$ was unsymmetrical, which indicated that there were two different valence states of silver in the catalysts. Fig. 6C shows the peak of Cl2p at 197.5 eV assigned to the Cl^- species in AgCl. The XPS results confirmed that the catalysts Ag-AgCl/WO_3 could be prepared by the deposition–precipitation–photoreduction method. From the TEM and XPS results, there was metallic silver in the as-prepared Ag-AgCl/WO_3 sample, implying that the excessive amount of silver might have been produced from the photo-reduction of AgCl on the surface. We calculated the ratios of Ag^0/Ag^+ using the classical chemical analysis method adopted in our previous work (Table 1) and found that the ratio of Ag^0/Ag^+ increased from 0.23 to 1.25 as the duration of photo-reduction increased from 10 to 40 min. The absolute amount of Ag^+ was determined by selectively dissolving the catalyst in aqueous solution of ammonia followed by chemical titration with KSCN, while the metallic silver kept stable and can be separated by filtration. In addition, the amount of metallic silver was obtained by dissolving the sample in diluted HNO_3 solution followed by chemical titration with KSCN. As to the sample 30Ag-AgCl/WO_3-500, the molar ratio of Ag/AgCl was 1.1 as determined by the XPS method, which was close to the value obtained by the classical chemical analysis method (0.91). As we know, XPS can present the surface character of catalysts and this finding was consistent well with the TEM results.

3.2. Photodegradation activity under visible light irradiation

Fig. 7 shows the photocatalytic activity of the Ag-AgCl/WO_3 prepared by different photoreduction duration. As shown, when being irradiated at wavelengths of $\lambda > 420$ nm under visible light, the reaction showed limited photocatalytic activity for the degradation of 4-CP without any catalysts or with WO_3 alone. However, the Ag-AgCl/WO_3 catalysts exhibited much higher photodegradation activity if compared with WO_3. Among the Ag-AgCl/WO_3 with different photoreduction duration, 30Ag-AgCl/WO_3 exhibited the highest photocatalytic activity. The photodegradation

Table 1
The Ag content of Ag-AgCl/WO_3-500 with different photo-reduction time.

Sample	Photoreduction time (min)	Ag content[a] (Ag/WO_3 wt.%)	Ag^0/Ag^+ [a]	Ag/Cl[b] Molar ratio
Ag/WO_3-500	30	3.2	–	–
AgCl/WO_3-500	0	3.1	–	0.9
10Ag-AgCl/WO_3-500	10	3.9	0.23	1.3
20Ag-AgCl/WO_3-500	20	3.8	0.72	1.3
30Ag-AgCl/WO_3-500	30	3.7	0.91	1.5
40Ag-AgCl/WO_3-500	40	3.8	1.25	1.7

[a] From AAS.
[b] Molar ratio determined by XPS.

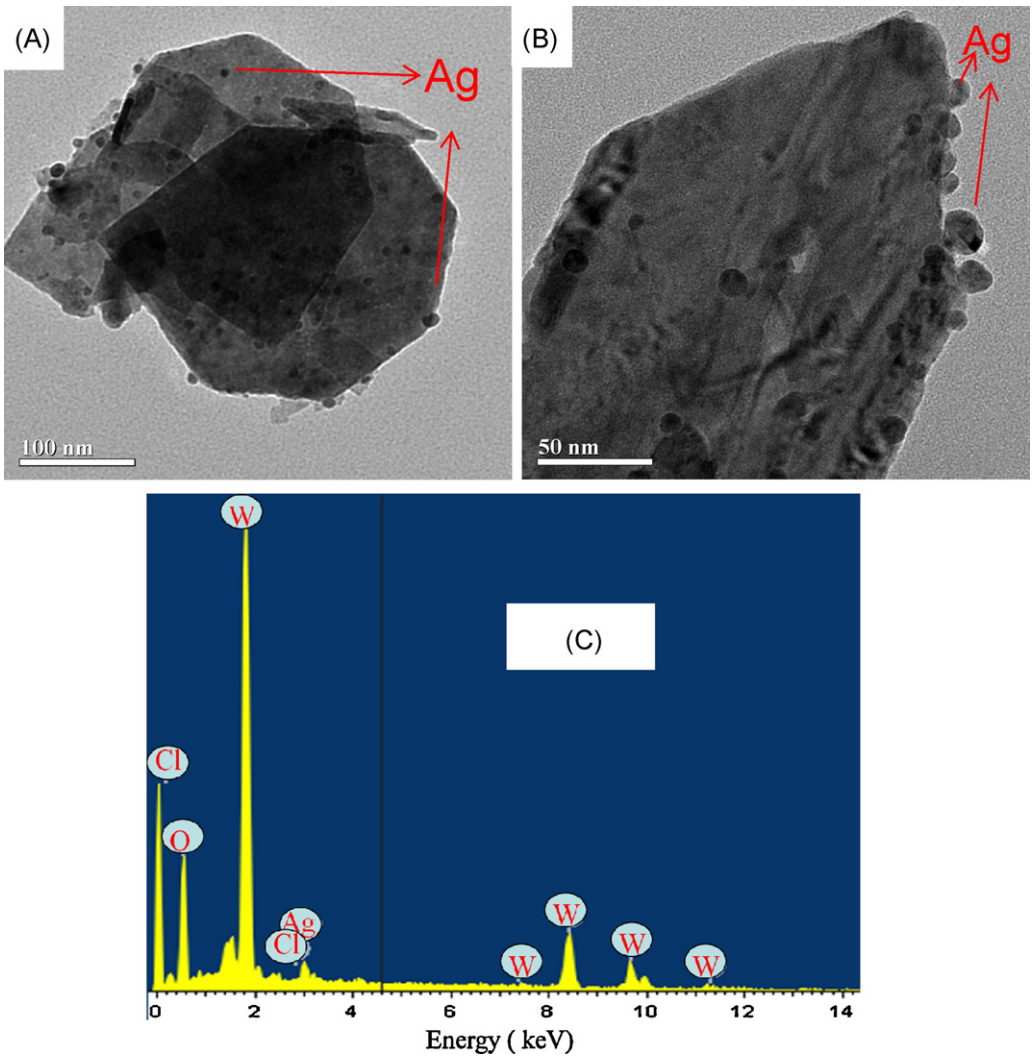

Fig. 5. TEM images (A and B) and EDX (C) of 30Ag-AgCl/WO_3 photocatalyst.

order is 30Ag-AgCl/WO_3 > 20Ag-AgCl/WO_3 > 40Ag-AgCl/WO_3 > 10Ag-AgCl/WO_3. Given that the degradation follows pseudo first order reaction, the degradation rate of 4-CP over 30Ag-AgCl/WO_3 was estimated to be 0.068 mg min^{-1}, while the degradation rate over WO_3 was 0.0058 mg min^{-1}, and the former was 11.7 times faster than the latter. According to the photodegradation order, it was demonstrated that the ratio of Ag and AgCl was a significant factor influencing the photodegradation rate. When the amount of metallic silver was very scarce, the generation of the electron–hole pairs on the metallic Ag may be decreased due to the SPR effect on the metallic Ag, and the active species was also cut down, which could reduce the photocatalytic activity. But when the amount of Ag was too high, some of the Ag nanoparticles became the active sites promoting the recombination of the photoelectrons and the holes, which also reduced the photocatalytic activity.

As for the degradation of 4-CP, Fig. 8 shows the photocatalytic activity of the four different kinds of catalysts. From this figure, it is found that, after being compared with the tungsten trioxide, the catalyst Ag/WO_3 showed limited effect on enhancing the photodegradation of 4-CP. Among the Ag/WO_3 catalysts, the photoexcited electrons produced on the silver nanoparticles due to the SPR effect may be transferred to the surface of WO_3, instead of absorbing O_2 to produce the active oxidation species. Yet, the electron produced on the surface of WO_3 can be trapped by Ag NPs, which enhanced the electron–hole pair separation and the photocatalytic activity of WO_3. At the beginning of the photodegradation of 4-CP over various AgCl/WO_3 catalysts, there was no obvious difference in their activity after being compared with WO_3 because AgCl was not likely to produce the photoelectrons and holes due to its big band gap at 3.2 eV. However, after 10 min reaction, the activity of AgCl/WO_3 was enhanced rapidly. Maybe Ag NPs was produced on the surface of AgCl. The results presented in Fig. 6 suggested that the coexistence of Ag and AgCl on the surface of WO_3 may cause the high photocatalytic activity when being irradiated by visible lights of $\lambda > 420$ nm. From the whole appraisal result of the photocatalytic activity, it was only the coexistence of Ag and AgCl on the surface of WO_3 that brought an excellent photocatalytic activity to the as-prepared catalysts. With the presence of AgCl, the active photoelectron on the silver nanoparticles due to SPR effect may be injected into the conduction band of WO_3 and transferred to the ubiquitous molecular oxygen to form the super-oxide radical O^{2-}, subsequently yielded the HOO• radicals through protonation, or then reacted with the trapped electrons to produce H_2O_2, finally HO• radicals also formed. All the active radicals can contribute to the decomposition of 4-CP. Simultaneously, electron–hole pairs photogenerated in Ag NPs due to SPR effect also could cause the oxidation of Cl^- ions into Cl^0 atoms, which were able to oxidize 4-CP and were reduced to Cl^- ions again. In one word, Ag and

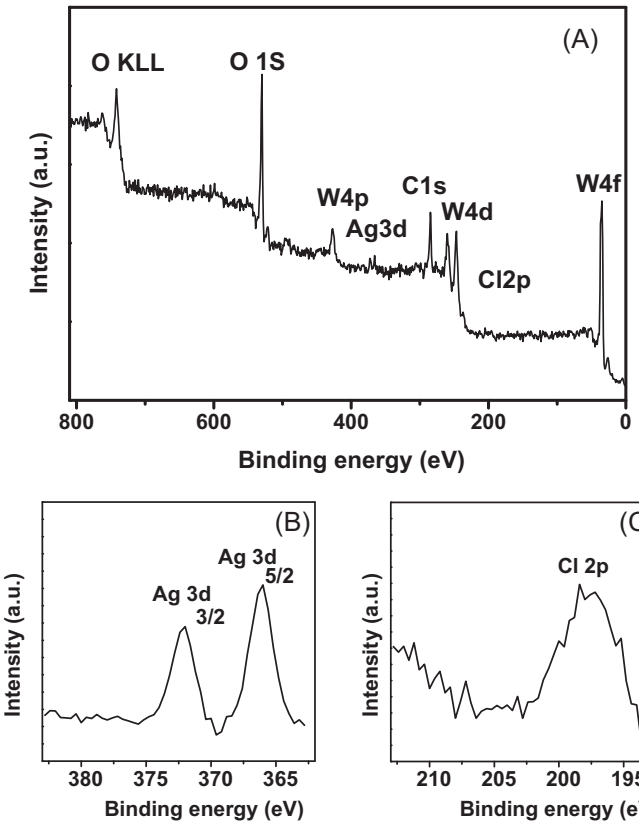

Fig. 6. XPS spectra of 30Ag-AgCl/WO_3 photocatalys (A) survey spectrum; (B) Ag 3d; (C) Cl 2p.

AgCl NPs are both indispensable to enhance the photocatalytic activity.

Prior to the activity test of the as-prepared samples, commercial P25 was tested as a reference, and it was found that P25 showed almost no photodegradation activity toward 4-CP under identical conditions. The hierarchical hollow shells not only possessed unique structure but also promoted the understanding and practical using of visible-light-driven plasmonic photocatalyst in the near future. It is well-known that the stability for a practical photocatalyst is very important as well as its photocatalytic activity. The plasmonic photocatalyst Ag-AgCl/WO_3 is further investigated by

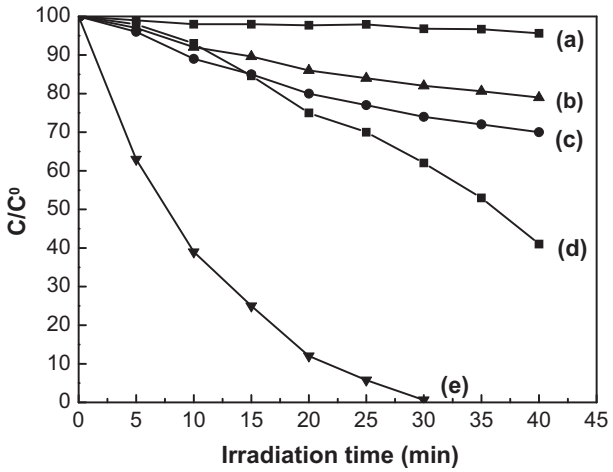

Fig. 8. Photodegradation of 4-CP in aqueous suspension under visible light irradiation over different photocatalysts (a) blank; (b) WO_3; (c) Ag/WO_3; (d) AgCl/WO_3; (e) 30Ag-AgCl/WO_3.

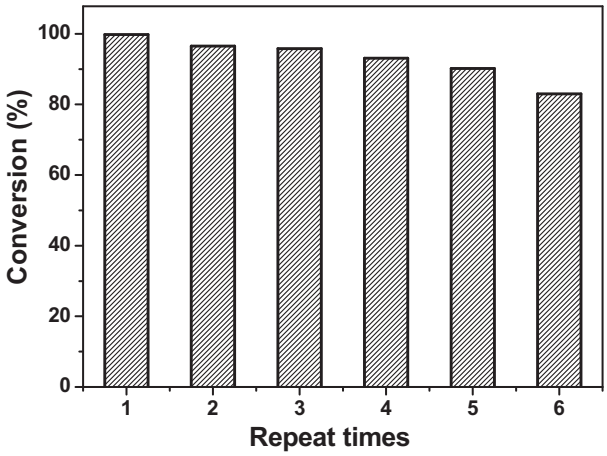

Fig. 9. Recycling test of 30Ag-AgCl/WO_3 under visible light irradiation.

the recycling experiments. As shown in Fig. 9, after six runs for the photodegradation of 4-CP, the sample did not show significant loss of photocatalytic activity, which indicated the catalyst remained stable during the photocatalytic reaction. We have performed the

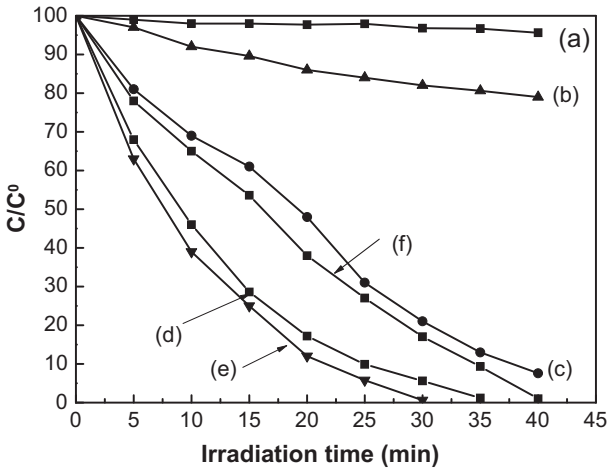

Fig. 7. Photodegradation of 4-CP in aqueous suspension under visible light irradiation over different photocatalysts (a) blank; (b) WO_3; (c) 10Ag-AgCl/WO_3; (d) 20Ag-AgCl/WO_3; (e) 30Ag-AgCl/WO_3; (f) 40Ag-AgCl/WO_3.

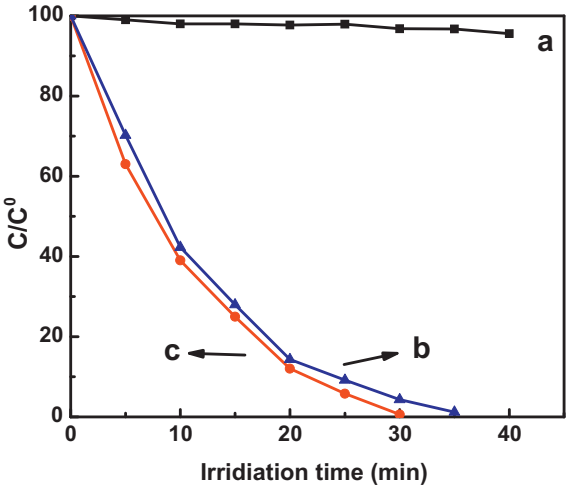

Fig. 10. Photodegradation of 4-CP in aqueous suspension under visible light irradiation over different photocatalysts (a) blank; (b) Ag-AgCl/WO_3-nanoparticles; (c) 30Ag-AgCl/WO_3-hollow sphere.

contrast experiments between the 30Ag-AgCl/WO_3 photocatalysts and Ag-AgCl/WO_3-nanoparticles. As shown in Fig. 10, obviously 30Ag-AgCl/WO_3-hollow sphere photocatalyst exhibited higher photocatalytic activity than the Ag-AgCl/WO_3-nanoparticles. This finding indicated that the structure, hollow sphere, definitely benefited the photocatalytic activity. All the above results indicate that the as-prepared Ag-AgCl/WO_3 is an active and stable visible-light-driven plasmonic catalyst, which may serve as a promising candidate for practical use in the degradation of pollutants. The studies of a detailed plasmon resonance effect induced photocatalytic mechanism are being under way.

4. Conclusions

In summary, the plasmonic Ag-AgCl/WO_3 hollow sphere, prepared by the deposition–precipitation–photoreduction method, exhibited a high photocatalytic activity for the degradation of 4-CP under visible light irradiation, and was quite stable after repeated use for more than 6 times. Because of the unique shape of the catalysts, the incident lights could be reflected repeatedly, which might enhance the utilization ratio of light so as to improve the photocatalytic activity of the as-prepared composites. Both the advantages of plasmon and composite effect have been combined to synthesize the novel semiconductor photocatalyst.

Acknowledgments

We thank the Major State Basic Resource Development Program (Grant No. 2012CB224804), NNSFC (Project 21173052, 20973042), the Research Fund for the Doctoral Program of Higher Education (20090071110011) and the Science & Technology Commission of Shanghai Municipality (08DZ2270500) for financial support.

References

[1] A. Fujishima, K. Honda, S. Kikuchi, Kogyo Kagaku Zasshi 72 (1969) 108–113.
[2] A. Fujishima, K. Honda, Nature 238 (1972) 37–38.
[3] C. Turchi, D. Ollis, Journal of Catalysis 122 (1990) 178–192.
[4] I. Konstantinou, T. Albanis, Applied Catalysis B: Environmental 49 (2004) 1–14.
[5] S. Liu, X. Chen, Journal of Hazardous Materials 152 (2008) 48–55.
[6] M.R. Elahifard, S. Rahimnejad, S. Haghighi, M.R. Gholami, Journal of the American Chemical Society 129 (2007) 9552–9553.
[7] Z.X. Lu, L. Zhou, Z.L. Zhang, W.L. Shi, Z.X. Xie, H.Y. Xie, D.W. Pang, P. Shen, Langmuir 19 (2003) 8765–8768.
[8] F. Iskandar, A.B.D. Nandiyanto, K.M. Yun, C.J. Hogan Jr., K. Okuyama, P. Biswas, Advanced Materials 19 (2007) 1408–1412.
[9] G. Wang, W. Lu, J.H. Li, J. Choi, Y. Jeong, S.Y. Choi, J.B. Park, M.K. Ryu, K. Lee, Small 2 (2006) 1436–1439.
[10] E. Allain, S. Besson, C. Durand, M. Moreau, T. Gacoin, J.-P. Boilot, Advanced Functional Materials 17 (2007) 549–554.
[11] Z. Bian, J. Zhu, S. Wang, Y. Cao, X. Qian, H. Li, Journal of Physical Chemistry C 112 (2008) 6258–6262.
[12] J. Zhang, F. Shi, J. Lin, D. Chen, J. Gao, Z. Huang, X. Ding, C. Tang, Chemistry of Materials 20 (2008) 2937–2941.
[13] S.U.M. Khan, M. Al-Shahry, W.B. Ingler Jr., Science 5590 (2002) 2243–2245.
[14] D. Matthey, J.G. Wang, S. Wendt, J. Matthiesen, R. Schaub, E.L. Sgaard, B. Hammer, F. Besenbacher, Science 5819 (2007) 1692–1696.
[15] H. Choi, A.C. Sofranko, D.D. Dionysiou, Advanced Functional Materials 16 (2006) 1067–1074.
[16] Y. Chen, J.C. Crittenden, S. Hackney, L. Sutter, D.W. Hand, Environmental Science and Technology 39 (2005) 1201–1208.
[17] H. Yu, X. Quan, S. Chen, H. Zhao, Journal of Physical Chemistry C 111 (2007) 12987–12991.
[18] M.K. Lee, T.H. Shih, Journal of the Electrochemical Society 154 (2007) 49–51.
[19] K. Awazu, M. Fujimaki, C. Rockstuhl, J. Tominaga, H. Murakami, Y. Ohki, N. Yoshida, T. Watanabe, Journal of the American Chemical Society 130 (2008) 1676–1680.
[20] P. Wang, B. Huang, X. Qin, X. Zhang, Y. Dai, J. Wei, M.H. Whangbo, Angewandte Chemie International Edition 47 (2008) 7931–7933.
[21] P. Wang, B. Huang, X. Zhang, X. Qin, H. Jin, Y. Dai, Z. Wang, J. Wei, J. Zhan, S. Wang, Chemical Engineering Journal 15 (2009) 1821–1824.
[22] N. Kakuta, N. Goto, H. Ohkita, T. Mizushima, Journal of Physical Chemistry B 103 (2009) 5917–5919.
[23] C. Hu, X. Hu, L. Wang, J. Qu, A. Wang, Environmental Science and Technology 40 (2006) 7903–7907.
[24] S. Rodrigues, S. Uma, I. Martyanov, Journal of Catalysis 233 (2005) 405–410.
[25] C. Hu, T. Peng, X. Hu, Y. Nie, X. Zhou, J. Qu, H. He, Journal of the American Chemical Society 132 (2010) 857–862.
[26] J. Guo, B. Ma, A. Yin, K. Fan, W. Dai, Applied Catalysis B: Environmental 101 (2011) 580–586.
[27] B. Ma, J. Guo, L. Zou, K. Fan, W. Dai, Chinese Journal of Chemistry 29 (2011) 857–859.
[28] D. Chen, J. Ye, Advanced Functional Materials 18 (2008) 1922–1928.
[29] S. Baeck, K. Choi, T.F. Jaramillo, G.D. Stucky, E.W. McFarland, Advanced Materials 15 (2003) 1269–1273.
[30] C. Santato, M. Odziemkowshi, M. Ulmann, J. Augustynski, Journal of the American Chemical Society 123 (2001) 10639–10649.
[31] Y. Baek, Y. Song, K.J. Yong, Advanced Materials 18 (2006) 3105–3110.
[32] Y. Oaki, H. Imai, Advanced Materials 18 (2006) 1807–1811.
[33] Z.X. Wang, S.X. Zhou, L.M. Wu, Advanced Functional Materials 17 (2007) 1790–1794.
[34] J. Thangala, S. Vaddiraju, R. Bogale, R. Thruman, T. Powers, B. Deb, M.K. Sunkara, Small 3 (2007) 890–896.
[35] Z.J. Gu, T.Y. Zhai, B.F. Gao, X.H. Sheng, Y.B. Wang, H.B. Fu, Y. Ma, J.N. Yao, Journal of Physical Chemistry B 110 (2006) 23829–23836.
[36] T. He, J. Yao, Journal of Materials Chemistry 17 (2007) 4547–4557.
[37] P. Agus, W. Hendri, O. Takashi, Catalysis Communications 12 (2010) 525–529.